J Physiol (2003), **550.1**, *pp.* 11–26
DOI: 10.1113/jphysiol.2003.036681

www.jphysiol.org

Journal of Physiology

Five ADNFLE mutations reduce the Ca^{2+} dependence of the mammalian $\alpha4\beta2$ acetylcholine response

Nivalda Rodrigues-Pinguet*†, Li Jia‡, Maureen Li*, Antonio Figl*, Alwin Klaassen§, Anthony Truong*, Henry A. Lester† and Bruce N. Cohen†

**Division of Biomedical Sciences, ‡Computer Science Department, University of California, Riverside, CA 92521-0121, §Psychiatry and Biobehavioral Sciences, University of California, Los Angeles, CA 90095-1759, and †Division of Biology, California Institute of Technology, Pasadena, CA 91125, USA*

Five nicotinic acetylcholine receptor (nAChR) mutations are currently linked to autosomal dominant nocturnal frontal lobe epilepsy (ADNFLE). The similarity of their clinical symptoms suggests that a common functional anomaly of the mutations underlies ADNFLE seizures. To identify this anomaly, we constructed rat orthologues (S252F, +L264, S256L, V262L, V262M) of the human ADNFLE mutations, expressed them in *Xenopus* oocytes with the appropriate wild-type (WT) subunit ($\alpha4$ or $\beta2$), and studied the Ca^{2+} dependence of their ACh responses. All the mutations significantly reduced 2 mM Ca^{2+}-induced increases in the 30 μM ACh response ($P < 0.05$). Consistent with a dominant mode of inheritance, this reduction persisted in oocytes injected with a 1:1 mixture of mutant and WT cRNA. BAPTA injections showed that the reduction was not due to a decrease in the secondary activation of Ca^{2+}-activated Cl^- currents. The S256L mutation also abolished 2 mM Ba^{2+} potentiation of the ACh response. The S256L, V262L and V262M mutations had complex effects on the ACh concentration–response relationship but all three mutations shifted the concentration–response relationship to the left at [ACh] > 30 μM. Co-expression of the V262M mutation with a mutation (E180Q) that abolished Ca^{2+} potentiation resulted in 2 mM Ca^{2+} block, rather than potentiation, of the 30 μM ACh response, suggesting that the ADNFLE mutations reduce Ca^{2+} potentiation by enhancing Ca^{2+} block of the $\alpha4\beta2$ nAChR. Ca^{2+} modulation may prevent presynaptic $\alpha4\beta2$ nAChRs from overstimulating glutamate release at central excitatory synapses during bouts of synchronous, repetitive activity. Reducing the Ca^{2+} dependence of the ACh response could trigger seizures by increasing $\alpha4\beta2$-mediated glutamate release during such bouts.

(Received 10 February 2003; accepted after revision 15 April 2003; first published online 16 May 2003)
Corresponding author B. N. Cohen, Division of Biology 156-29, California Institute of Technology, Pasadena, CA 91125, USA.
Email: bncohen@caltech.edu

Autosomal dominant nocturnal frontal lobe epilepsy (ADNFLE) patients suffer from brief, partial epileptic seizures that appear to originate in the frontal lobe and occur almost exclusively during phase 2 sleep (Scheffer *et al.* 1995). Three $\alpha4$ (Steinlein *et al.* 1995, 1997; Hirose *et al.* 1999) and two $\beta2$ nicotinic acetylcholine receptor (nAChR) mutations (DeFusco *et al.* 2000; Phillips *et al.* 2001) are currently linked to ADNFLE. All five mutations lie within (or immediately adjacent to) M2, the putative pore-forming region of the nAChR subunits (reviewed in Karlin *et al.* 1995), and they produce similar clinical symptoms (Steinlein *et al.* 1995, 1997; Hirose *et al.* 1999; DeFusco *et al.* 2000; Ito *et al.* 2000; Phillips *et al.* 2001). Previous studies have shown that the ADNFLE mutations have a range of effects on the $\alpha4\beta2$ ACh response (reviewed in Sutor *et al.* 2001). However, the similarity of their clinical symptoms suggests that a common functional anomaly of the mutations generates ADNFLE seizures.

Previous studies have reported that several ADNFLE mutations have common effects on the $\alpha4\beta2$ ACh response. The human $\alpha4$(S248F), $\alpha4$(776ins3), $\alpha4$(S252L) and $\beta2$(V287M) ADNFLE mutations shift the ACh concentration–response relationship to the left (Bertrand *et al.* 2002). Rat orthologues (S252F, +L264) of the human $\alpha4$(S248F) and $\alpha4$(776ins3) mutations induce use-dependent potentiation of the 100 nM ACh response, delay the rising phase of the 5–30 nM ACh response, and reduce 2.5 mM Ca^{2+}-induced increases in the peak 30 μM ACh response (Figl *et al.* 1998). The human $\alpha4$(S248F) mutation also displays use-dependent potentiation (Kuryatov *et al.* 1997) and the human $\alpha4$(776ins3) mutation reduces 2.5 mM Ca^{2+} potentiation of the peak 30 μM ACh response (Steinlein *et al.* 1997). However, it is unclear whether use-dependent potentiation, delays in the rising phase of the 5–30 nM ACh response, and reductions in the Ca^2 dependence of the ACh response are common features of all the ADNFLE mutations.

We constructed rat orthologues (S256L, V262L, V262M) of the human α4(S252L), β2(V287L) and β2(V287M) mutations (Fig. 1*A* and *B*) and co-expressed them in *Xenopus* oocytes with the appropriate wild-type (WT) subunit to determine whether use-dependent potentiation, delays in the rising phase of the 5–30 nM ACh response and reductions in Ca^{2+} potentiation were common features of the ADNFLE mutations. The rat (Goldman *et al.* 1987; Deneris *et al.* 1988) and human (Anand *et al.* 1990; Monteggia *et al.* 1995) α4 and β2 amino acid sequences share 89 % and 95 % identity, respectively. Their β2 M2 sequences are identical (Fig. 1*B*). The α4 M2 sequences differ by a single conservative amino acid substitution (I ⟷ V) at position 1′ (Fig. 1*A*).

Our results show that the S256L mutation does not induce use-dependent potentiation or delay the rising phase of the 10 nM ACh response. Thus, these effects are not common features of the ADNFLE mutations. In contrast, all five ADNFLE mutations reduce 2 mM Ca^{2+}-induced increases in the peak 30 μM ACh response and this reduction is consistent with a dominant mode of inheritance. During bouts of synchronous repetitive activity, reducing the Ca^{2+} dependence of presynaptic α4β2 nAChRs could induce seizures by increasing the relative amount of α4β2-mediated glutamate release at central excitatory synapses.

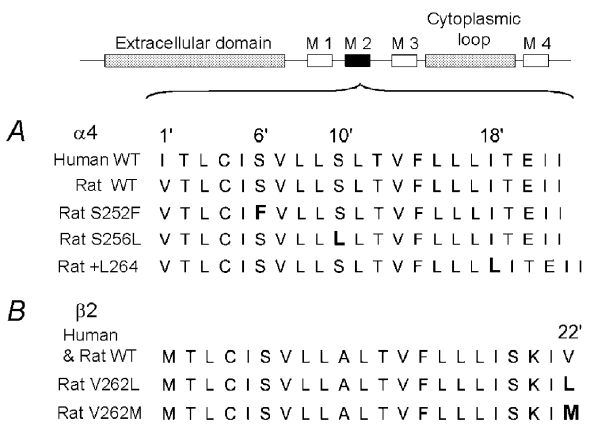

Figure 1. Locations of the autosomal dominant nocturnal frontal lobe epilepsy (ADNFLE) mutations

The block diagram above *A* indicates the nicotinic subunit domains. *A*, the aligned amino acid sequences of the rat and human wild-type (WT), and the rat S252F, S256L and +L264 M2 domains. The rat and human WT α4 M2 sequences differ by a single amino acid at position 1. *B*, alignment of the rat and human WT, and rat V262L and V262M β2 M2 domains, as in *A*. The rat and human WT β2 M2 sequences are identical. The mutated residues are shown in bold. The primed numbers above the sequences indicate the position of the residue relative to the amino (N)-terminus (position 1′) of M2 (Charnet *et al.* 1990).

METHODS

Oocyte expression

Stage V–VI *Xenopus* oocytes were surgically isolated following previously published protocols (Quick *et al.* 1994*a*). All surgeries were in done in compliance with the methods approved by the Institutional Animal Care and Use Committee (IACUC) at the California Institute of Technology. Ovarian lobes were removed from female *Xenopus laevis* anaesthetized by immersion in 0.2 % tricaine methanesulphonate (pH 7.4; Sigma, St Louis, MO, USA) for 45–60 min. *Xenopus* were humanely killed after the final oocyte extraction. The oocyte follicular layer was removed using Type A collagenase (1–2 h in a 2 mg ml^{-1} collagenase solution; Boehringer Mannheim, Indianapolis, IN, USA). To increase receptor expression, the α4-1(Goldman *et al.* 1987) and β2 inserts (Deneris *et al.* 1988) were subcloned into a vector containing a 5′ untranslated region from the alfalfa mosaic virus that enhanced protein translation, and a long 3′ poly A tail (Figl *et al.* 1998). We used the Stratagene QuikChange kit (La Jolla, CA, USA) to construct the α4 and β2 mutations, and verified them by DNA sequencing. Capped cRNA was synthesized *in vitro* using the mMessage mMachine RNA transcription kit (Ambion, Austin, TX, USA). After a 24 h incubation in a modified Barth's solution containing (mM): NaCl 96, Hepes 5, sodium pyruvate 2.5, KCl 2, $CaCl_2$ 1.8 and $MgCl_2$ 1 with 2.5 μg ml^{-1} gentamicin (Sigma) and 5 % horse serum (pH 7.4, Irvine Scientific, Santa Ana, CA, USA), the isolated oocytes were injected with rat α4 and β2 cRNA, or mouse thyrotrophin-releasing hormone receptor (TRHr) cRNA. The injected oocytes were incubated for ⩾ 24 h in the modified Barth's solution at 15 °C before electrophysiological recordings or [^{3}H]epibatidine binding measurements were attempted.

Electrophysiological recordings

We voltage clamped the oocytes with two, 3 MΩ KCl-filled microelectodes (1.5–4 MΩ resistance) at −50 mV using a GeneClamp voltage clamp (Axon Instruments, Union City, CA, USA). During the voltage-clamp recordings, the oocytes were continually superfused with a nominally Ca^{2+}-free saline solution (ND98) containing (mM): NaCl 98, $MgCl_2$ 1 and Hepes 5 (pH 7.4) at 20–23 °C, unless otherwise stated. We added 2 mM $CaCl_2$ to the ND98 to measure the Ca^{2+} dependence of the α4β2 ACh response and 2 mM $BaCl_2$ to measure its Ba^{2+} dependence. We used a concentration of 2 mM Ca^{2+} rather than the previously used 2.5 mM (Steinlein *et al.* 1997; Figl *et al.* 1998) because the extracellular Ca^{2+} concentration in the mammalian brain is 1.5–2 mM (reviewed in Egelman *et al.* 1999). ACh was applied to the oocytes using a U-tube microperfusion system (Cohen *et al.* 1995). The time constant for solution exchange was ~0.5 s. The voltage-clamp currents were digitized with a personal computer equipped with a DigiData 1200 A/D interface and pCLAMP V.6.03 software (Axon Instruments). To avoid aliasing, the voltage-clamp currents were filtered at one-quarter to one-third of the sampling frequency with an 8-pole, low-pass Bessel filter. Unless otherwise stated, we used Student's unpaired *t* tests to determine whether two independent groups of measurements were significantly different, and the Student-Newman-Keuls test (SigmaStat V.1, Jandel Scientific) for multi-group comparisons. All the normalized ACh concentration–response data were fitted initially to the Hill equation. If the Hill coefficient from this initial fit was < 0.8, then the data were refitted to the sum of two hyperbolic binding functions (equivalent to the sum of two Hill equations with both Hill coefficients fixed to unity). If the Hill coefficient was 0.8–1.0, then the data were refitted to a single hyperbolic binding function.

BAPTA injections

The oocytes were injected with 50 nl of a BAPTA solution containing (mM): BAPTA 100, NaOH 85, KOH 2.5 and Hepes 10 (pH 7.4), 5 min before the recordings began, to prevent activation of the endogenous Ca^{2+}-activated Cl^- current by the TRHr or $\alpha4\beta2$ nAChR (Haghighi *et al.* 2000). The BAPTA injections produced a final intracellular BAPTA concentration of ~5 mM. Control oocytes were injected with 50 nl of sterile water.

[^{3}H]Epibatidine binding to immunoisolated receptors

We purchased [^{3}H]epibatidine (specific activity of 30–50 Ci mmol^{-1}) from Amersham Life Science, Inc. (Arlington Heights, IL, USA). The WT and S256L [^{3}H]epibatidine concentration–binding relationships were measured as in Shafaee *et al.* (1999), except that the $\alpha4\beta2$ nAChRs were incubated for 12 h in [^{3}H]epibatidine in the current experiments. Oocytes expressing $\alpha4\beta2$ nAChRs were solubilized in a lysis buffer containing (mM): NaCl 50, sodium phosphate buffer 50, EGTA 5 and EDTA 5 with 2% Triton X-100 and the Complete protease inhibitor (1 tablet per 40 ml of lysis buffer, Boehringer Mannheim; Gerzanich *et al.* 1995). The solubilized receptors were immunoprecipitated onto EIA/RIA strip plates (Costar Corning Corp., Cambridge, MA, USA) coated with the anti-$\alpha4$ antibody mAb 299 (Research Biochemicals, Natick, MA, USA). The wells were coated with antibody the previous day by adding 0.5 μg of mAb 299 to 100 μl of a 10 mM sodium bicarbonate solution (pH 8.8) for an overnight incubation at 4 °C. We blocked the antibody-coated wells with bovine serum albumin (3%) in 200 μl of a PBS–Tween buffer containing (mM): NaCl 10 and sodium phosphate 100 with 0.05% Tween 20 (pH 7.5) for 2 h at 4 °C. The blocked wells were rinsed three times with the PBS–Tween buffer. Aliquot parts of the solubilized receptor in lysis buffer (100 μl) were added to each well and incubated overnight at 4 °C. On the following day, the wells were rinsed three times with the PBS–Tween buffer and the appropriate [^{3}H]epibatidine concentration was added to each well in PBS–Tween buffer for 12 h at 20–23 °C. This incubation time was $\geqslant$ 20 times longer than the [^{3}H]epibatidine dissociation time constant for rat $\alpha4\beta2$ receptors expressed in oocytes (Shafaee *et al.* 1999). To avoid radioligand depletion, we adjusted the amount of receptor in the wells to keep the bound [^{3}H]epibatidine to within 10% or less of the total [^{3}H]epibatidine added. Incubation volumes of 4 ml were used for [^{3}H]epibatidine concentrations of 0.001–0.3 nM. Volumes of 200 μl were used for [^{3}H]epibatidine concentrations > 0.3 nM. The free [^{3}H]epibatidine concentration was corrected for radioligand depletion. Non-specific binding was measured by adding 1 mM cold (−)nicotine to the wells. Non-specific binding was negligible (near background radiation levels) except for 30 nM [^{3}H]epibatidine. Each measurement was repeated three times. We added 2–3 ml of liquid scintillation cocktail (Research Products International Corp., Mount Prospect, IL, USA) to each sample and measured the amount of [^{3}H]epibatidine bound using a scintillation counter. To obtain the equilibrium dissociation constant (K_d) for [^{3}H]epibatidine binding and the maximum bound [^{3}H]epibatidine (B_{max}), we fitted the [^{3}H]epibatidine concentration–binding data to a hyperbolic binding function using the non-linear least squares regression routine in SigmaPlot V. 4 (SPSS, Chicago, IL, USA).

[^{3}H]Epibatidine binding to intact oocytes

We used nearly saturating [^{3}H]epibatidine (10 nM) and unlabelled ACh concentrations (1 mM) to measure WT and S256L surface receptor expression in intact oocytes. Half of the oocytes were used to measure total [^{3}H]epibatidine binding and half of them were used to measure non-specific binding. To measure total [^{3}H]epibatidine binding, we incubated individual oocytes in 200 μl of ND98 (see above) containing 10 nM [^{3}H]epibatidine for 2 min at 20–23 °C. This incubation time minimized [^{3}H]epibatidine uptake by the oocytes but was sufficient for 10 nM [^{3}H]epibatidine binding to the receptors to approach equilibrium (Shafaee *et al.* 1999). To measure non-specific binding, we incubated individual oocytes in 200 μl of ND98 containing 10 nM [^{3}H]epibatidine and 1 mM ACh for 2 min. ACh is a hydrophilic quaternary amine that cannot readily cross the cell membrane and, thus, selectively blocks [^{3}H]epibatidine binding to surface nAChRs. After the incubations, each group of oocytes was rinsed three times in 10 ml ND98 and solubilized individually overnight in 200 μl concentrated nitric acid. We added 2 ml scintillation fluid to each sample and measured the amount of [^{3}H]epibatidine bound using a scintillation counter.

RESULTS

S256L does not induce use-dependent potentiation or delay the rising phase of the ACh response

Previous experiments have shown that the rat S252F and +L264 mutations induce use-dependent potentiation of the 100 nM ACh response and prolong the rise time of the 5–30 nM ACh response (Figl *et al.* 1998). To determine whether the S256L mutation had similar effects on the

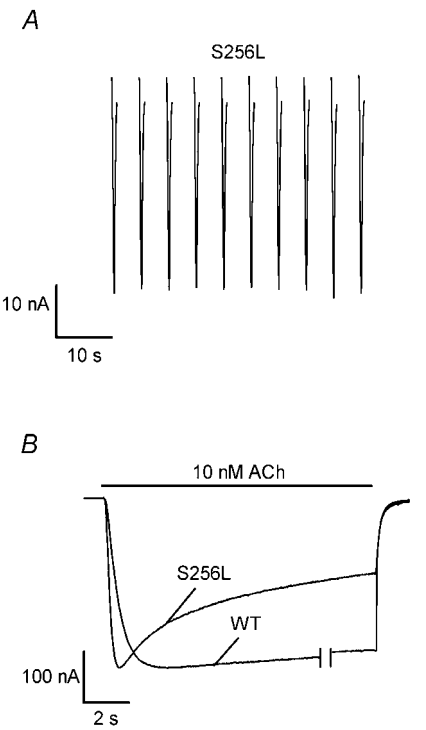

Figure 2. The S256L mutation does not induce use-dependent potentiation of the 100 nM ACh response or delay the rising phase of the 10 nM ACh response

A, traces showing the inward currents evoked by applying ten, 150 ms pulses of 100 nM ACh spaced 5 s apart to an oocyte expressing S256L receptors. *B*, normalized WT and S256L 10 nM ACh responses on an expanded time scale. A portion of the WT response between the double vertical lines was omitted to align the beginning and end of the WT and S256L responses. The bars above the traces indicate the timing of the ACh application.

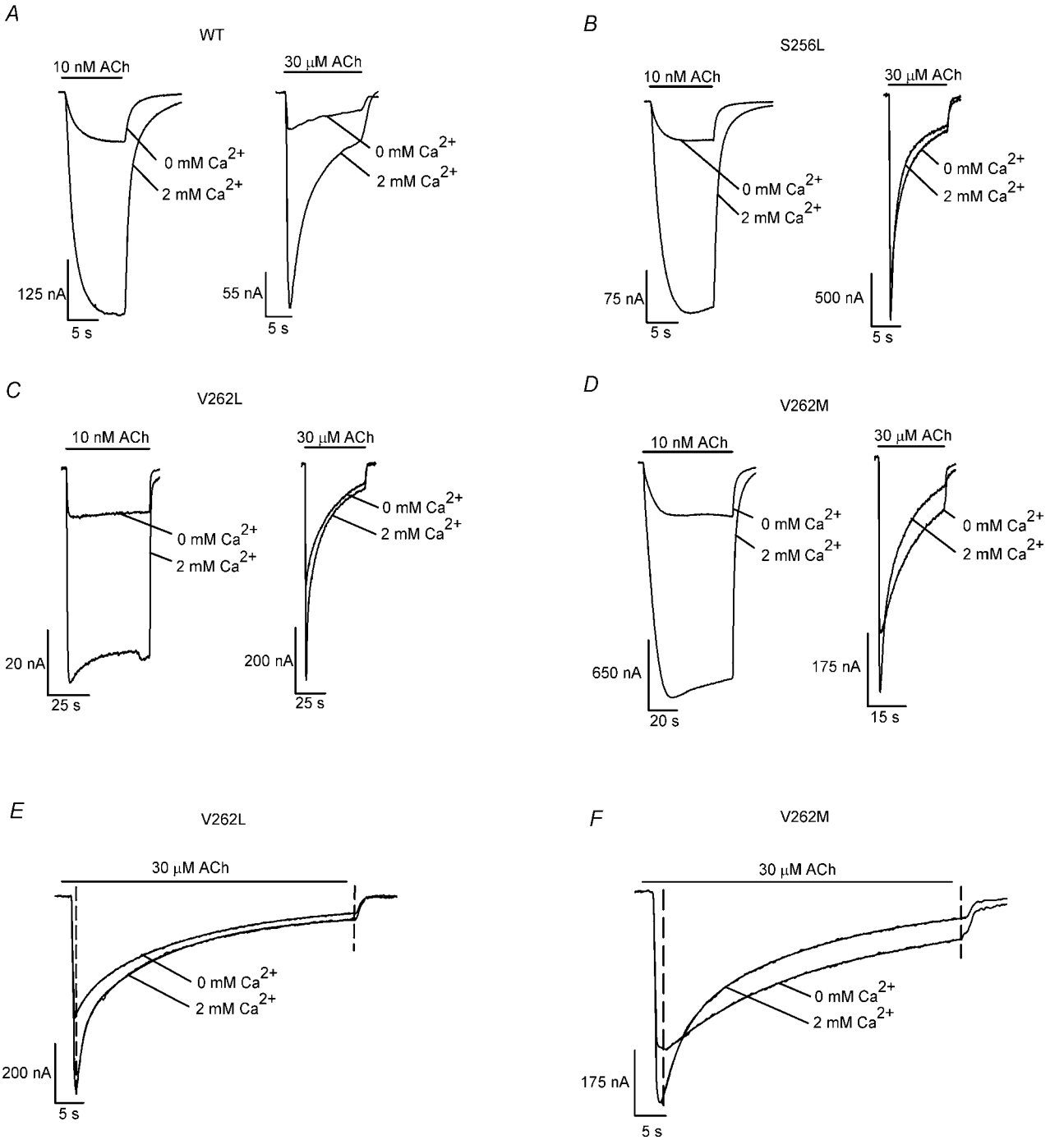

Figure 3. S256L, V262L and V262M reduce the Ca^{2+} dependence of the 30 μM ACh response

The traces show the WT (*A*), S256L (*B*), V262L (*C*) and V262M (*D*) 10 nM and 30 μM ACh responses in 0 and 2 mM added extracellular Ca^{2+} (n = 3–16 oocytes). Adding 2 mM Ca^{2+} to the saline solution increased the peak WT 10 nM and 30 μM ACh response by similar factors. It also increased the peak WT (*A*), S256L (*B*), V262L (*C*) and V262M (*D*) 10 nM ACh responses by similar factors. In contrast, adding 2 mM Ca^{2+} to the saline solution increased the peak S256L (*B*), V262L (*C*) and V262M (*D*) 30 μM ACh responses two- to 3-fold less than the WT response (*A*). The rise times of the ACh responses are somewhat slower than those in Fig. 2 because the rate of solution exchange was slower. The 10 nM and 30 μM ACh data in *A*–*D* were obtained from different oocytes. To avoid saturating the voltage clamp, we recorded the 30 μM ACh responses 1–2 days after cRNA injection and the 10 nM ACh responses 4–5 days after injection. *E* and *F*, the V262L (*E*) and V262M (*F*) 30 μM ACh responses are shown on an expanded time scale to facilitate comparison with the WT (*A*) and S256L (*B*) 30 μM ACh responses. Fits to the sum of two exponentials and a constant term (between the dashed lines) are superimposed on the responses. The mean ± S.E.M. fast (τ_f) and slow (τ_s) time constants, amplitudes of the fast (I_f) and slow (I_s) exponential components, and amplitude of the steady-state component (I_{ss}) for the V262L responses were 3.00 ± 0.04 s, 21.0 ± 0.1 s, 71 ± 1 nA 304 ± 1 nA, and

Table 1. Mean fractional amplitudes and mean τ values for WT, S256L, V262L and V262M receptors

	$[Ca^{2+}]$ (mM)	A_f (%)	A_s (%)	A_{ss} (%)	τ_f (s)	τ_s (s)
WT ($n = 25$)	0	16 ± 1	48 ± 2	36 ± 3	3.4 ± 0.4	34 ± 4
S256L ($n = 7$)	0	37 ± 3*	53 ± 2	10 ± 1*	0.9 ± 0.1*	4 ± 1*
V262L ($n = 14$)	0	19 ± 3	66 ± 5	14 ± 4*	3 ± 1	19 ± 2*
V262M ($n = 6$)	0	23 ± 7	64 ± 8	13 ± 3*	5 ± 3	24 ± 6
WT ($n = 14$)	2	33 ± 6†	38 ± 4	29 ± 4	1.8 ± 0.3	24 ± 4
S256L ($n = 4$)	2	46 ± 4	43 ± 3	11 ± 2*	0.5 ± 0.1*	3.2 ± 0.3*
V262L ($n = 10$)	2	58 ± 5*†	40 ± 4	1 ± 3*	1.8 ± 0.3	21 ± 4
V262M ($n = 3$)	2	50 ± 5†	47 ± 5	3 ± 1*	2 ± 1	20 ± 5

All values are means ± S.E.M. *$P < 0.05$, significantly different from the corresponding WT value. †$P < 0.05$, significantly different from the corresponding value in 0 mM Ca^{2+}.

ACh response, we used the same protocol and perfusion system (U-tube) for these experiments (Fig. 2*B*) that we used previously for the S252F and +L264 experiments (Figl *et al.* 1998). In contrast to the S252F and +L264 mutations (Figl *et al.* 1998), the S256L mutation failed to exhibit use-dependent potentiation during a series of ten 150 ms applications of 100 nM ACh spaced 5 s apart (Fig. 2*A*). These experiments were replicated three times. Likewise, the S256L mutation failed to delay the rising phase of the 10 nM ACh response (Fig. 2*B*). On the contrary, the S256L mutation accelerated the rising phase of the 10 nM ACh response, presumably because it increased the rate of ACh-induced desensitization (Bertrand *et al.* 2002; Matsushima *et al.* 2002). These experiments were replicated seven times. The superposition of the normalized WT and S256L responses after the ACh application ceased (Fig. 2*B*) shows that the difference between the rising phases of the WT and S256L responses was not the result of a difference in the rate of solution exchange. We did not carry out similar experiments on the V262L or V262M receptors because we were only interested in common effects of the five reported ADNFLE mutations.

S256L, V262L and V262M reduce Ca^{2+} modulation of the 30 μM ACh response

Similar to the S252F and +L264 mutations (Figl *et al.* 1998), the S256L mutation also reduced Ca^{2+}-induced increases in the peak 30 μM ACh response compared with WT (Fig. 3*A* and *B*). The effects of the S256L mutation on Ca^{2+} modulation of the ACh response depended on the agonist concentration (Fig. 3*A* and *B*). Removing 2 mM Ca^{2+} from the saline solution had little effect on the peak 30 μM ACh response of the S256L mutation but it had WT-like effects on the peak 10 nM ACh response of the mutation (Fig. 3*A* and *B*). The V262L and V262M mutations had similar effects on Ca^{2+} modulation of the ACh response (Fig. 3*C–F*). Thus, all three mutations dramatically reduced 2 mM Ca^{2+}-induced increases in the 30 μM ACh response but they had little effect on 2 mM Ca^{2+}-induced increases in the 10 nM ACh response.

S256L, V262L and V262M enhance steady-state desensitization

To compare desensitization of the WT and mutant receptors, we fitted the desensitizing phase of the WT, S256L, V262L and V262M 30 μM ACh responses to the sum of two exponentials and a constant term (Table 1, Fig. *3E* and *F*). Table 1 gives the fast (τ_f) and slow (τ_s) desensitization time constants, the fractional amplitudes of fast (A_f) and slow (A_s) desensitization components, and the fractional amplitude of the steady-state response (A_{ss}) for the mutant and WT receptors. A two-way analysis of variance (using receptor type and Ca^{2+} concentration as factors) showed that the S256L, V262L and V262M mutations significantly ($P < 0.05$) increased steady-state desensitization of the 30 μM ACh response (i.e. reduced the A_{ss}). The mutant A_{ss} values were 51–72 % lower than the WT value in 0 mM Ca^{2+} and 62–97 % lower than the WT value in 2 mM Ca^{2+} (Table 1). However, S256L, V262L and V262M did not uniformly affect the other desensitization parameters (τ_f, τ_s, A_f and A_s). S256L significantly affected the τ_f for desensitization ($P < 0.05$) but V262L and V262M did not. S256L reduced the τ_f by 74 % in 0 mM Ca^{2+} and 72 % in 2 mM Ca^{2+}, compared to the WT. S256L and V262L significantly reduced the τ_s for desensitization ($P < 0.05$) but V262M did not. The S256L τ_s was 88 % lower than the WT value in 0 mM Ca^{2+} and 87 % lower in 2 mM Ca^{2+}. The V262L τ_s was 44 % lower than the WT value in 0 mM Ca^{2+} but it was not significantly

30 ± 1 nA in 0 mM Ca^{2+}, and 1.00 ± 0.01 s, 16 ± 1 s, 231 ± 1 nA, 360 ± 1 nA and 63 ± 1 nA in 2 mM Ca^{2+}. The corresponding V262M values were 18 ± 2 s, 50 ± 20 s, 190 ± 60 nA, 210 ± 40 nA and 40 ± 20 nA in 0 mM Ca^{2+}, and 4.0 ± 0.01 s, 30 ± 1 s, 249 ± 5 nA, 332 ± 2 nA and 6 ± 6 nA in 2 mM Ca^{2+}. The bars above the traces indicate the timing of the ACh applications.

different from the WT value in 2 mM Ca^{2+}. S256L increased the A_f by ~2-fold in 0 mM Ca^{2+} but had no significant effect in 2 mM Ca^{2+}. In contrast, V262L increased the A_f by ~2-fold in 2 mM Ca^{2+} but had no significant effect in 0 mM Ca^{2+}. None of the mutations significantly affected the A_s. Adding 2 mM Ca^{2+} to the saline solution also had divergent effects on desensitization. A two-way analysis of variance showed that adding 2 mM Ca^{2+} to the saline solution had a significant overall effect on the τ_f, A_f, A_s and A_{ss} ($P < 0.05$). Ca^{2+} significantly increased the WT, V262L and V262M A_f values by 2- to 3-fold but did not significantly affect the S256L A_f. However, *post hoc* comparisons between the τ_f, A_s and A_{ss} in 0 and 2 mM Ca^{2+} failed to show any significant differences. Finally, Ca^{2+} did not significantly affect the τ_s. Thus, the only uniform effect of the mutations on desensitization of the 30 μM ACh response was an increase in steady-state desensitization.

Not all the mutations affect Ca^{2+} modulation in an ACh-dependent manner

To determine whether all five ADNFLE mutations reduced 2 mM Ca^{2+} modulation in an ACh concentration-dependent manner, we measured the ratio ($I_{Ca^{2+}}/I_0$) between the peak ACh response in 2 and 0 mM added Ca^{2+} for the WT, S252F, +L264, S256L, V262L and V262M receptors at three ACh concentrations (10 nM, 50 nM, 30 μM) (Fig. 4). All five mutations significantly reduced the $I_{Ca^{2+}}/I_0$ ratio of the 30 μM ACh response ($P < 0.05$). The WT $I_{Ca^{2+}}/I_0$ ratio at 30 μM ACh was 4.9 ± 0.4 ($n = 16$). (This value was greater than the previously reported $I_{Ca^{2+}}/I_0$ ratio of 2.9 ± 0.4 between 0 and 2.5 mM Ca^{2+} (Figl *et al.* 1998), probably because the ACh responses in the nominally Ca^{2+}-free saline solution in the previous experiments were potentiated by residual Ca^{2+} in the water.) The mutant $I_{Ca^{2+}}/I_0$ ratios at 30 μM ACh ranged from 1.4 ± 0.1 ($n = 4$) to 2.5 ± 0.1 ($n = 5$). They were 50–72 % lower than the WT value but were not significantly different from each other. The S252F and +L264 mutations significantly reduced the $I_{Ca^{2+}}/I_0$ ratio at 10 nM and 50 nM ACh ($P < 0.05$). In contrast, the S256L, V262L and V262M mutations did not, although the S256L and V262M $I_{Ca^{2+}}/I_0$ ratios at 50 nM ACh were smaller than the corresponding WT value (Fig. 4). Thus, all five ADNFLE mutations reduced 2 mM Ca^{2+}-induced increases in the peak 30 μM ACh response but only the S252F and +L264 mutations significantly reduced 2 mM Ca^{2+}-induced increases in the 10 and 30 nM ACh responses.

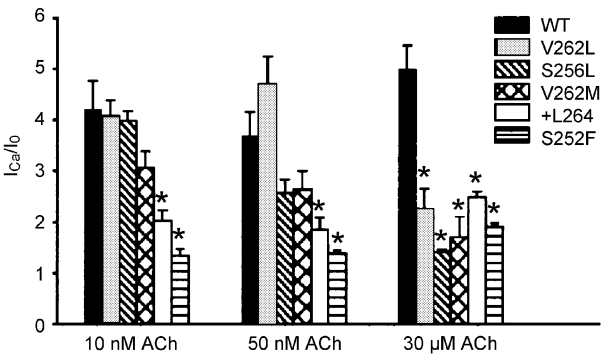

Figure 4. All the rat ADNFLE orthologues significantly reduce the Ca^{2+} dependence of the 30 μM ACh response

The bars denote the ratio ($I_{Ca^{2+}}/I_0$) of the peak 10 nM, 50 nM and 30 μM ACh response in 2 mM added Ca^{2+} to that in 0 mM added Ca^{2+}. The error bars are ±S.E.M. (n = 3–16 oocytes). The asterisks denote a significant difference from the corresponding WT values ($P < 0.05$). To normalize the $I_{Ca^{2+}}/I_0$ distribution, we ranked the ratios and took the square roots of the ranks. *Post hoc* comparisons were carried out on the square root of the ranks using the Student-Newman-Keuls test.

Ba^{2+} blocks the S256L mutation

Ba^{2+} also acts as a positive allosteric modulator of neuronal nAChRs (Mulle *et al.* 1992). However, it is far less effective than Ca^{2+} at activating Cl^- currents in *Xenopus* oocytes (Miledi *et al.* 1984). To determine whether the S256L mutation affected Ba^{2+} modulation of the $\alpha4\beta2$ ACh response, we measured the WT and S256L 30 μM ACh response in zero and 2 mM extracellular Ba^{2+}. Adding 2 mM Ba^{2+} to the saline solution increased the peak amplitude of the WT 30 μM ACh response by a factor of 1.20 ± 0.06 (Fig. 5*A*). In contrast, it reduced that of the S256L receptor by 16 ± 3 % ($n = 7$; Fig. 5*A* and *B*). The ratio between the peak WT 30 μM ACh response in 2 mM and 0 mM Ba^{2+} (1.20 ± 0.06, $n = 5$) was significantly greater ($P < 0.01$) than that of the S256L receptor (0.84 ± 0.03, $n = 7$). Thus, the S256L mutation not only eliminated the 2 mM Ba^{2+}-induced increase in the peak 30 μM ACh response but also resulted in Ba^{2+} block of the receptor. Ba^{2+} is not a physiological cation. Thus, we did not carry out similar experiments with the other ADNFLE mutations.

Ca^{2+}-induced increases in the ACh response are not an artifact of Cl^- currents

Ca^{2+} influx through the WT and mutant $\alpha4\beta2$ nAChRs could potentially activate endogenous Ca^{2+}-activated Cl^-

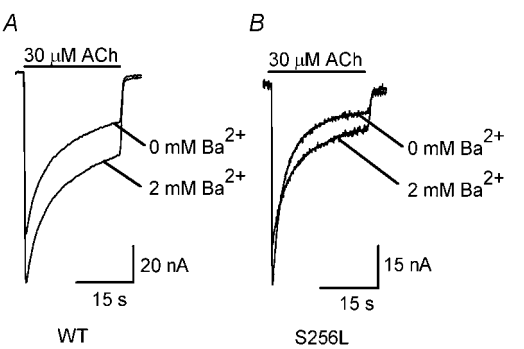

Figure 5. Ba^{2+} (2 mM) blocks the S256L 30 μM ACh response

WT (*A*) and S256L (*B*) responses to 30 μM ACh in 0 and 2 mM Ba^{2+}. Bars above the traces show the timing of the ACh applications.

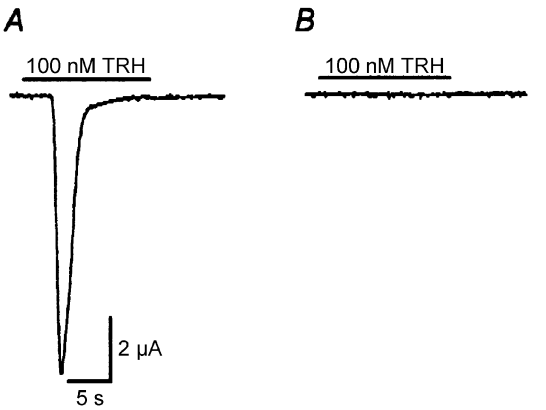

Figure 6. BAPTA injections completely eliminate the response of the TRHr to 100 nM TRH

A, the application of 100 nM TRH evoked a peak inward current of 12.2 ± 2.5 μA (mean + S.E.M., $n = 3$ oocytes) in water-injected oocytes (see Methods). *B*, BAPTA-injected oocytes did not respond to 100 nM TRH ($n = 6$ oocytes). The bars above the traces indicate the timing of the TRH application.

currents in *Xenopus* oocytes. Therefore, we used BAPTA injections (Kavanaugh *et al.* 1991; Wadiche *et al.* 1995; Haghighi *et al.* 2000) to determine whether the secondary activation of Ca^{2+}-activated Cl^- currents made a significant contribution to the 2 mM Ca^{2+}-induced increases in the WT and mutant receptor ACh responses. Mouse TRHrs expressed in oocytes activate Cl^- currents by triggering intracellular Ca^{2+} release (Quick *et al.* 1994*b*). To test the effectiveness of the BAPTA injections, we expressed mouse TRHrs in oocytes and examined the effects of BAPTA injections on the TRH response. After verifying that BAPTA injections completely blocked the TRH response (Fig. 6*A* and *B*), we examined their effects on 2 mM Ca^{2+}-induced increases in the WT and V262M ACh responses (Fig. 7*A–D*). BAPTA injections reduced 2 mM Ca^{2+}-induced increases in the WT response by a small, but insignificant, amount (Fig. 7*A* and *B*). The $I_{Ca^{2+}}/I_0$ ratio of the WT 30 μM ACh response was 5.0 ± 0.7 ($n = 4$) for the water-injected controls (Fig. 7*A*) and 3.8 ± 0.3 for the BAPTA-injected oocytes ($n = 5$; Fig. 7*B*). The BAPTA

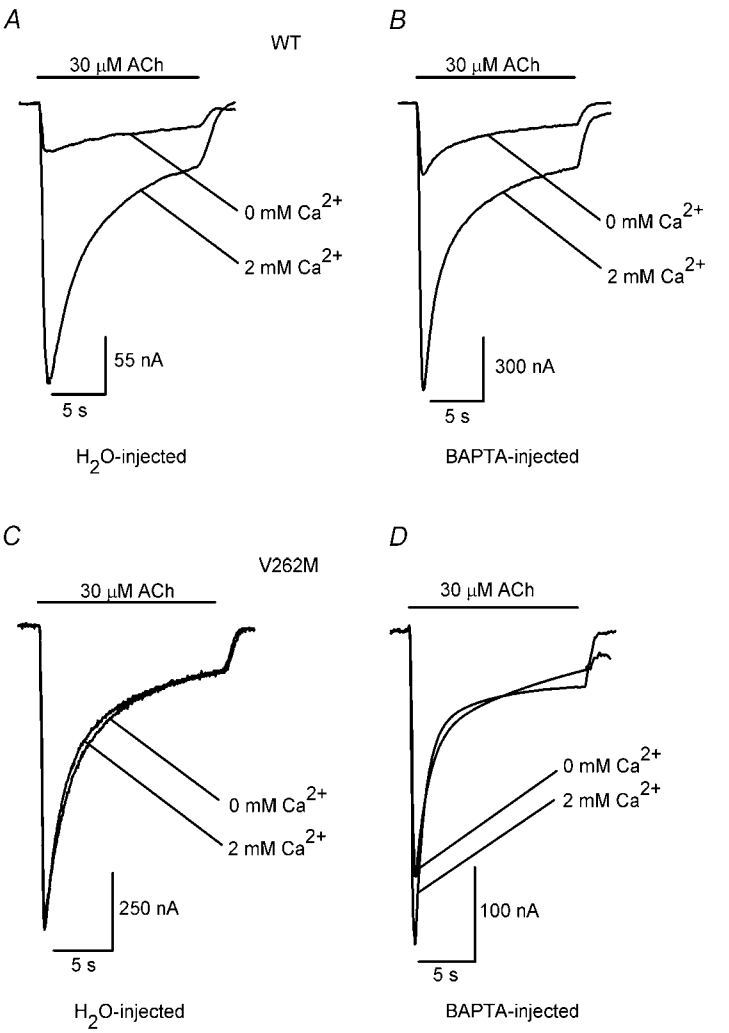

Figure 7. BAPTA injections do not significantly affect 2 mM Ca^{2+}-induced increases in the peak WT and V262M 30 μM ACh response

The traces denote the WT (*A* and *B*) and V262M 30 μM ACh responses (*C* and *D*) in 0 and 2 mM added extracellular Ca^{2+}. The oocytes were injected with 50 nl of water (*A* and *C*) or 5 mM BAPTA (*B* and *D*) before the recordings. The bars above the traces indicate the timing of the ACh application.

injections also failed to significantly affect Ca^{2+}-induced increases in the V262M ACh response (Fig. 7*C* and *D*). The $I_{Ca^{2+}}/I_0$ ratio of the V262M 30 μM ACh response was 1.3 ± 0.1 ($n = 4$) for the water-injected controls (Fig. 7*C*) and 1.1 ± 0.1 ($n = 5$) for the BAPTA-injected oocytes (Fig. 7*D*). Thus, the secondary activation of Ca^{2+}-activated Cl^- currents by $\alpha4\beta2$-mediated Ca^{2+} influx did not contribute significantly to 2 mM Ca^{2+}-induced increases in the WT and V262M 30 μM ACh responses.

The mutant effects on Ca^{2+} modulation are consistent with dominant inheritance

ADNFLE segregates in an autosomal dominant fashion (reviewed in Hirose *et al.* 2000). To determine whether the ADNFLE mutations reduced the Ca^{2+} dependence of the $\alpha4\beta2$ ACh response in a dominant fashion, we measured the 2 mM Ca^{2+}-induced increases in the peak WT, S256L, V262M and mock heterozygous receptor 1 mM ACh responses. We did not test the V262L, S252F and +L264 mutants. We used 1 mM ACh in these experiments to ensure maximum receptor activation. Since the $\alpha4$:$\beta2$ subunit stoichiometry is expected to be 2:3 in central nicotinic receptors, we examined heterozygous conditions using an ADNFLE mutation present in the $\alpha4$ subunit and one present in the $\beta2$ subunit. To mimic the homozygous condition, the oocytes were injected with S256L $\alpha4$ and WT $\beta2$ cRNA in a 2:3 $\alpha4$:$\beta2$ ratio, or with WT $\alpha4$ and V262M $\beta2$ cRNA in the same $\alpha4$:$\beta2$ ratio. To mimic the heterozygous condition, oocytes were injected with WT $\alpha4$, S256L $\alpha4$, and WT $\beta2$ cRNA in a 1:1:3 $\alpha4$:$\alpha4$:$\beta2$ ratio or, with WT $\alpha4$, WT $\beta2$ and V262M $\beta2$ cRNA in a 2:1.5:1.5 $\alpha4$:$\beta2$:$\beta2$ ratio. The $I_{Ca^{2+}}/I_0$ ratio of the WT 1 mM ACh response (3.2 + 0.3, $n = 6$; Fig. 8*A*) was within the range of the $I_{Ca^{2+}}/I_0$ ratios for the 10 nM, 50 nM and 30 μM ACh WT responses (from 3.6 ± 0.4 to 4.9 ± 0.4). The S256L and V262M mutations reduced the $I_{Ca^{2+}}/I_0$ ratio by comparable amounts in the heterozygous and homozygous conditions (Fig. 8*B*–*E*). The heterozygous S256L $I_{Ca^{2+}}/I_0$ ratio (1.5 ± 0.5, $n = 4$; Fig. 8*B*) was not significantly different

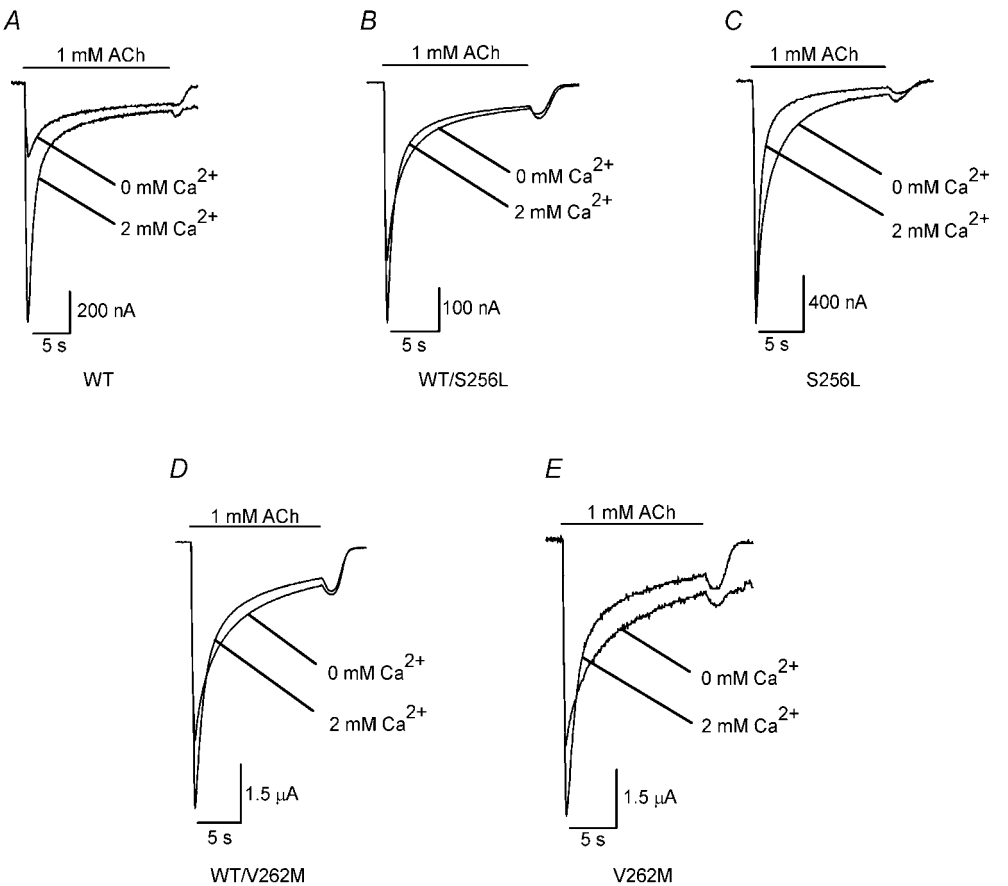

Figure 8. Heterozygous expression of the S256L and V262M mutations reduces the Ca^{2+} dependence of the 1 mM ACh response by nearly the same amount as homozygous expression

WT (*A*), heterozygous S256L (WT/S256L, *B*), homozygous S256L (*C*), heterozygous V262M (WT/V262M, *D*), and homozygous V262M (*E*) responses to 1 mM ACh in 0 and 2 mM added extracellular Ca^{2+}. The bar above the traces shows the timing of the ACh application. The small rebound currents at the end of the ACh applications suggest that, at a concentration of 1 mM, ACh has a slight open-channel blocking effect on the WT and mutant channels.

from the homozygous ratio (1.0 ± 0.03, $n = 3$; Fig. 8*C*). Similarly, the heterozygous V262M $I_{Ca^{2+}}/I_0$ ratio (1.9 ± 0.2, $n = 4$; Fig. 8*D*) was not significantly different from the V262M homozygous ratio (1.8 ± 0.2, $n = 3$; Fig. 8*E*). Thus, the S256L and V262M mutations reduced the Ca^{2+} dependence of the ACh response in a manner consistent with dominant inheritance.

S256L, V262L and V262M mutations increase ACh sensitivity at [ACh] ⩾ 30 μM

To determine whether the S256L, V262L or V262M mutations affected ACh sensitivity, we measured the WT and mutant ACh concentration–response relationships at −50 mV (Fig. 9). Consistent with previous studies (Covernton *et al.* 2000; Buisson & Bertrand, 2001), the WT, S256L and V262L ACh concentration–response data were best fitted by the sum of two hyperbolic binding functions. In contrast, the V262M data were adequately fitted by a single hyperbolic binding function. Visual inspection of the data in Fig. 9*G* shows that all three mutations appear to shift the concentration–response relationship to the left at ACh concentrations ⩾ 30 μM. The high-affinity EC_{50}, low-affinity EC_{50} and percentage of

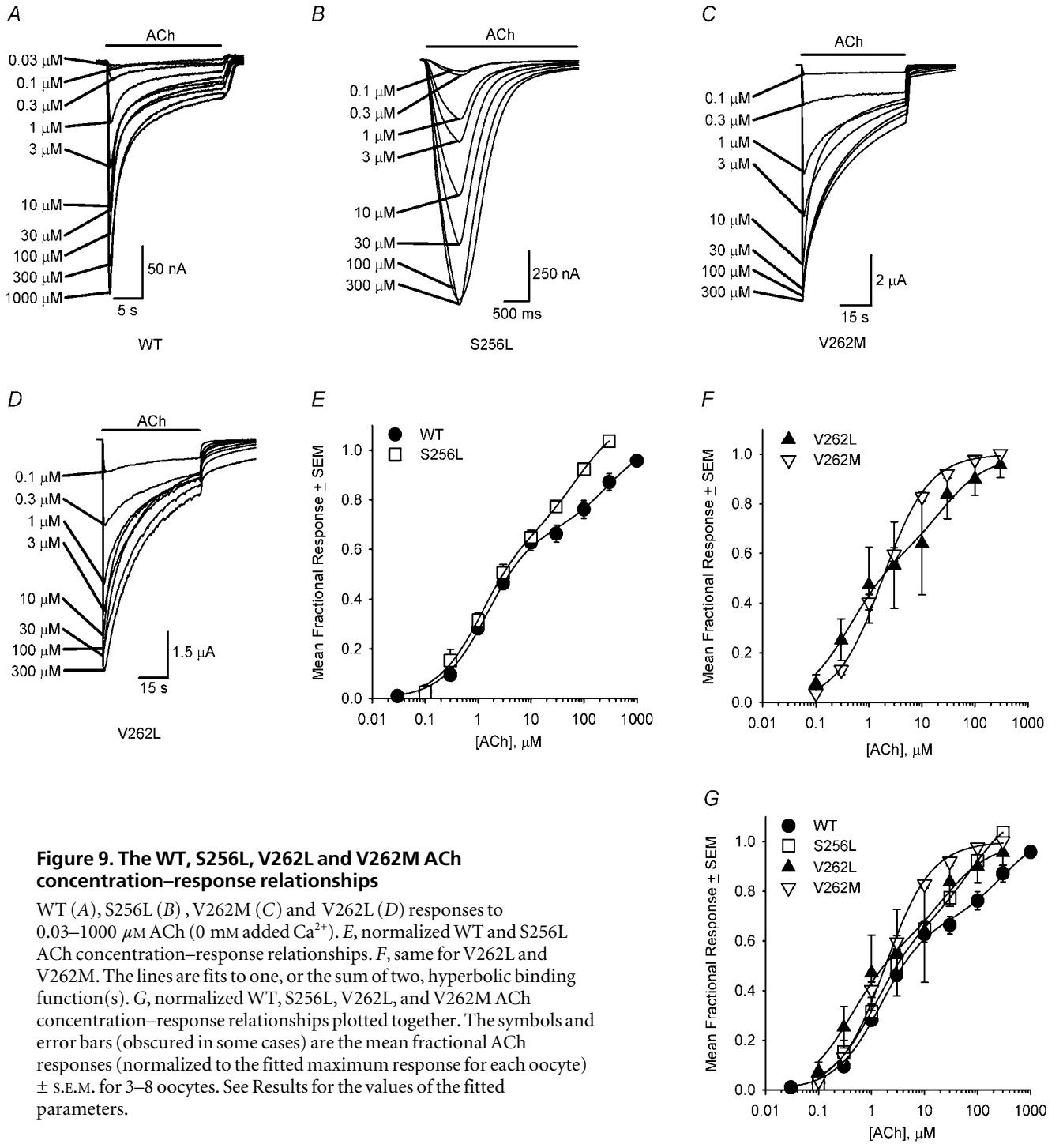

Figure 9. The WT, S256L, V262L and V262M ACh concentration–response relationships

WT (*A*), S256L (*B*) , V262M (*C*) and V262L (*D*) responses to 0.03–1000 μM ACh (0 mM added Ca^{2+}). *E*, normalized WT and S256L ACh concentration–response relationships. *F*, same for V262L and V262M. The lines are fits to one, or the sum of two, hyperbolic binding function(s). *G*, normalized WT, S256L, V262L, and V262M ACh concentration–response relationships plotted together. The symbols and error bars (obscured in some cases) are the mean fractional ACh responses (normalized to the fitted maximum response for each oocyte) ± S.E.M. for 3–8 oocytes. See Results for the values of the fitted parameters.

high-affinity receptors for the WT ACh concentration–response relationship were 1.5 ± 0.2 μM, 300 ± 130 μM and 67 ± 3 % (means ± S.E., degrees of freedom (d.f.) = 6), respectively (Fig. 9*E* and *G*). These values were similar to those (1.6 ± 0.2 μM, 62 ± 8.3 μM, 62 ± 3 %) reported for the human WT $\alpha4\beta2$ ACh concentration–response relationship at −100 mV (Bertrand *et al.* 2002). The V262L mutation significantly reduced the high- and low-affinity EC_{50} values (0.42 ± 0.16 μM, 25 ± 20 μM, d.f. = 4) but it did not significantly affect the percentage of high-affinity receptors (59 ± 9 %; Fig. 9*F* and *G*). The S256L mutation did not significantly affect the high-affinity EC_{50}, low-affinity EC_{50}, or percentage of high-affinity receptors (1.2 ± 0.2 μM, 80 ± 30 μM and 59 ± 4 %, d.f. = 4; Fig. 9*E* and *G*). The EC_{50} of the V262M concentration–response relationship (1.8 ± 0.1 μM, d.f. = 7) was not significantly different from the high-affinity WT or S256L EC_{50} values. However, the V262M concentration–response relationship lacked a noticeable low-affinity component (Fig. 9*F* and *G*). Thus, the S256L, V262L and V262M mutations had divergent effects on the ACh concentration–response relationship but all three mutations appeared to increase the fractional response to non-saturating ACh concentrations ⩾ 30 μM. Previous results (Fig. 4*D* in Figl *et al.* 1998) have shown that the S252F and +L264 mutations also shift the ACh concentration–response relationship to the left at ACh concentrations ⩾ 10 μM ACh, although these mutations only marginally affect the EC_{50}.

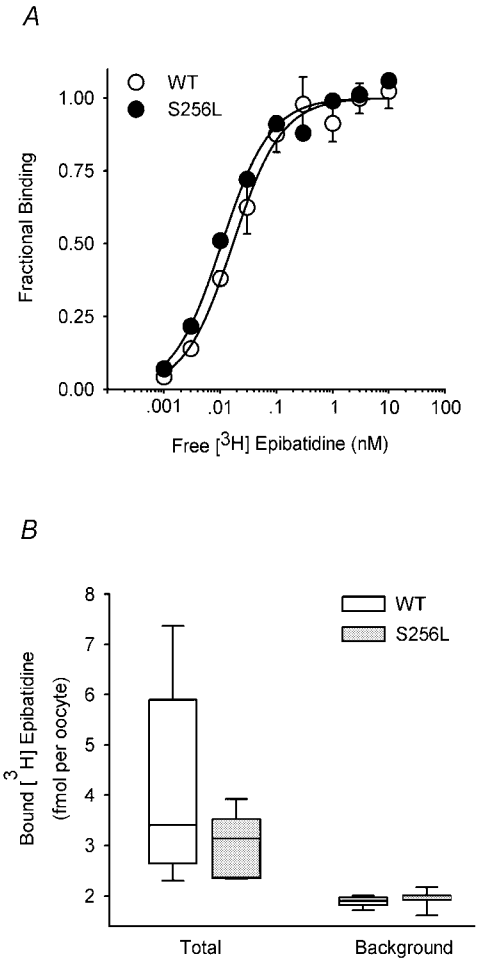

Figure 10. The S256L mutation has little effect on the [^{3}H]epibatidine affinity of $\alpha4\beta2$ nAChRs or their surface expression

A, normalized WT and S256L [^{3}H]epibatidine concentration–binding relationships. The symbols and error bars (obscured in some cases) are the mean fractional binding (normalized to the fitted B_{max}) ± S.E.M. (n = 3 replicates). The smooth lines are fits to a simple hyperbolic binding function. See Results for the values of the fitted parameters. *B*, box plot showing the total and background [^{3}H]epibatidine bound to intact oocytes expressing WT or S256L receptors. The total [^{3}H]epibatidine bound to the WT and S256L nAChRs was significantly greater than background binding ($P < 0.05$, Kruskal-Wallis one-way analysis of variance on ranks). The lines inside the boxes are medians (n = 9–11 oocytes per group). The box boundaries closest to the median are the 25th percentiles. Those farthest away are the 75th percentiles. The error bars below and above the box indicate the 10th and 90th percentiles, respectively.

S256L has little effect on [^{3}H]epibatidine affinity or surface receptor expression

To determine whether the S256L mutation affected the K_d or B_{max} of [^{3}H]epibatidine binding, we injected oocytes with equal amounts of receptor cRNA, immunoisolated the expressed WT or S256L receptors with mAb 299 and measured their [^{3}H]epibatidine concentration–binding relationships (see Methods). Consistent with previous results for the S252F and +L264 mutations (Figl *et al.* 1998), the S256L mutation did not have a major effect on the [^{3}H]epibatidine affinity of desensitized $\alpha4\beta2$ nAChRs. The normalized WT and S256L [^{3}H]epibatidine concentration–binding relationships were nearly superposed (Fig. 10*A*). The WT and S256L K_d values were 17 ± 2 pM and 11 ± 1 pM (d.f. = 7), respectively. The WT K_d was somewhat smaller than the value (30 ± 6 pM) previously measured for high-affinity rat WT $\alpha4\beta2$ receptors expressed in *Xenopus* oocytes (Shafaee *et al.* 1999). The S256L B_{max} (581 ± 12 c.p.m., d.f. = 7) was larger than the WT value (296 ± 5 c.p.m., d.f. = 7), suggesting that the S256L mutation increased total receptor expression ~2-fold. However, the S256L mutation did not significantly affect surface receptor expression (Fig. 10*B*). The median [^{3}H]epibatidine bound to surface WT receptors in intact oocytes was 3.4 fmol(oocyte)$^{-1}$ (2.7 and 5.8 fmol (oocyte)$^{-1}$ for 25th and 75th percentiles, respectively) and that bound to surface S256L receptors was 3.1 fmol (oocyte)$^{-1}$ (2.4 and 3.5 fmol (oocyte)$^{-1}$ for 25th and 75th percentiles, respectively). Because changes in surface expression or [^{3}H]epibatidine affinity were not common features of the ADNFLE mutations, we did not perform similar experiments with the V262M and V262L mutations.

V262M enhances Ca^{2+} block of the $\alpha4\beta2$ nAChR

Previous experiments show that a mutation (E172Q) in the N-terminal domain of $\alpha7$ nAChRs completely

eliminates Ca^{2+} potentiation of the ACh response (Galzi *et al.* 1996) and that 10–20 mM Ca^{2+} blocks the human $\alpha4\beta2$ ACh response (Buisson *et al.* 1996). To determine whether the ADNFLE mutations reduced the Ca^{2+} dependence of the $\alpha4\beta2$ ACh response by enhancing Ca^{2+} block, we made an $\alpha4$ mutation (E180Q) orthologous to E172Q, co-expressed it with the WT $\beta2$ subunit or the V262M mutation, and measured the effects of 2 mM Ca^{2+} on the peak 30 μM ACh responses of the single E180Q and double E180Q/V262M mutations. Consistent with the effects of the orthologous $\alpha7$ mutation (Galzi *et al.* 1996), co-expression of the E180Q mutation with the WT $\beta2$ subunit completely eliminated 2 mM Ca^{2+}-induced increases in the 30 μM ACh response (Fig. 11*A*). The $I_{Ca^{2+}}/I_0$ of the E180Q 30 μM ACh response was 0.85 ± 0.05 ($n = 7$). Moreover, co-expression of E180Q and V262M resulted in Ca^{2+} block, rather than potentiation, of the 30 μM ACh response (Fig. 11*B*). The $I_{Ca^{2+}}/I_0$ of the E180Q/V262M 30 μM ACh response was 0.60 ± 0.01 (mean ± S.E.M., $n = 4$ oocytes). This value was significantly less than the corresponding E180Q $I_{Ca^{2+}}/I_0$ ratio ($P < 0.01$). Thus, adding 2 mM Ca^{2+} to the saline solution reduced the peak E180Q/V262M 30 μM ACh response by 40 %. However, neither the E180Q mutation itself, nor the combination of the E180Q and V262M mutations, affected the ACh concentration–response relationship significantly (Fig. 11*C–E*). The E180Q and E180Q/V262M ACh concentration–response data were best fitted by the sum of two hyperbolic binding functions. The high-affinity EC_{50}, low-affinity EC_{50} and percentage of high-affinity receptors for the E180Q ACh

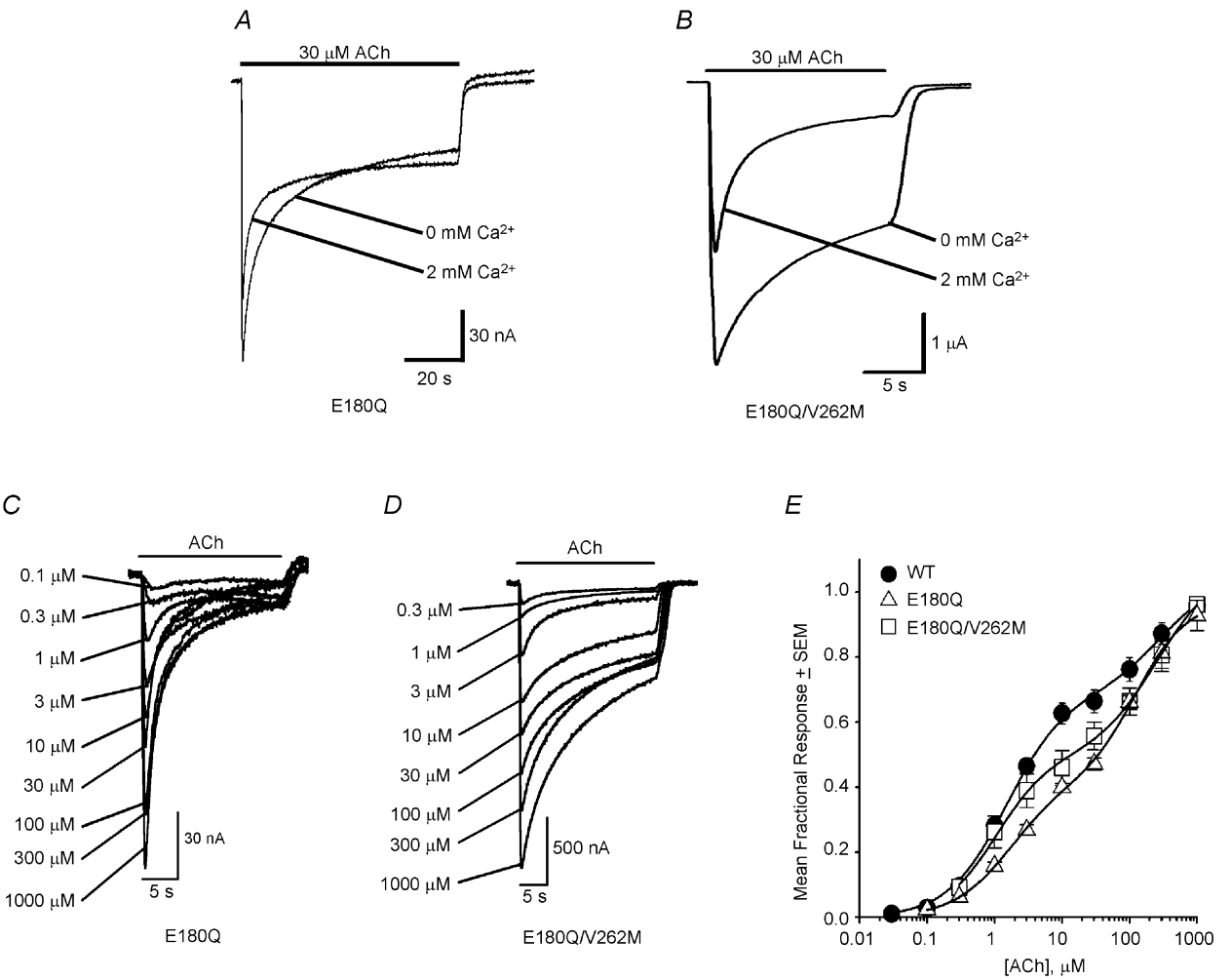

Figure 11. Ca^{2+} (2 mM) blocks the E180Q/V262M 30 μM ACh response

A and *B*, the E180Q response (*A*) and the E180Q/V262M response (*B*) to 30 μM ACh in the presence and absence of 2 mM added Ca^{2+}. The oocytes were injected with 5 mM BAPTA prior to recording. *C* and *D*, the E180Q (*C*) and E180Q/V262M (*D*) responses to 0.1–1000 μM ACh. The bar above the traces in *A–D* indicates the timing of the ACh application. *E*, normalized WT, E180Q and E180Q/V262M ACh concentration–response relationships. The lines are fits to the sum of two hyperbolic binding functions using non-linear least-squares regression. The symbols and error bars (obscured in some cases) are the mean fractional ACh responses (normalized to the fitted maximum response for each oocyte) ± S.E.M. for 3–4 oocytes. See Results for the values of the fitted parameters.

concentration–response relationship were 1.6 ± 0.2 μM, 128 ± 20 μM and 60 ± 2 % (mean ± S.E., d.f. = 6), respectively. The corresponding values for the E180Q/V262M double mutation were 1.1 ± 0.2 μM, 260 ± 65 μM and 57 ± 4 %. Thus, the V262M mutation reduced the Ca^{2+} dependence of the $\alpha4\beta2$ ACh response by enhancing Ca^{2+} block of the receptor. The effects of Ca^{2+} on combinations of the E180Q and other ADNFLE mutations (S252F, +L264, S256L, V262M) were not tested.

DISCUSSION

The five currently reported ADNFLE mutations have at least one common effect on the $\alpha4\beta2$ ACh response. They all reduce 2 mM Ca^{2+}-induced increases in the peak 30 μM ACh response. The mutant ratios between the 30 μM ACh response in 2 and 0 mM Ca^{2+} are 50–72 % less than the WT value. Consistent with these results, previous experiments show that the human $\alpha4$(776ins3) mutation also reduces the ratio between the peak 30 μM ACh response in 2.5 and 0 mM Ca^{2+} by a similar amount (Steinlein *et al.* 1997). The effects of the ADNFLE mutations on the Ca^{2+} dependence of the $\alpha4\beta2$ ACh response are consistent with a dominant mode of inheritance and they appear to be mediated by an enhancement of Ca^{2+} block of the receptor. Similar to +L264 and S256L mutations (Figl *et al.* 1998), the S256L mutation has little effect on the [^{3}H]epibatidine affinity of desensitized receptors. Moreover, the S256L mutation does not affect surface receptor expression.

A reduction in $\alpha4\beta2$ Ca^{2+} permeability cannot explain the effects of the ADNFLE mutations on Ca^{2+}-induced increases in the ACh response. First, not all the ADNFLE mutations reduce Ca^{2+} permeability. The human $\alpha4$(S248F) mutation reduces $\alpha4\beta2$ Ca^{2+} permeability (Kuryatov *et al.* 1997) but the $\alpha4$(776ins3) does not (Bertrand *et al.* 2002). Second, BAPTA injections show that Ca^{2+}-activated Cl^- currents do not make a significant contribution to 2 mM Ca^{2+}-induced increases in the WT ACh response. Thus, even a total loss of $\alpha4\beta2$ Ca^{2+} permeability cannot explain the effects of the ADNFLE mutations on 2 mM Ca^{2+}-induced increases in the 30 μM ACh response.

A gain of function generates ADNFLE seizures

The absence of seizures in $\alpha4$ (Marubio *et al.* 1999) and $\beta2$ knock-out mice (Picciotto *et al.* 1998), and the ability of carbamazepine (an $\alpha4\beta2$ antagonist) to block ADNFLE seizures (Picard *et al.* 1999), suggests that a gain of $\alpha4\beta2$ function underlies ADNFLE seizures. Postsynaptic Ca^{2+}-permeable glutamate channels at central excitatory synapses appear to act as Ca^{2+} sinks that deplete Ca^{2+} from the limited extracellular space surrounding the synapse during bouts of synchronous repetitive firing (Vassilev *et al.* 1997; Rusakov *et al.* 2003). Under these circumstances, the reduced Ca^{2+} sensitivity of the ADNFLE mutations could produce a net gain of $\alpha4\beta2$ function. The resulting increase in $\alpha4\beta2$-stimulated glutamate release could generate seizures.

The effects of the $\alpha4$(S248F) mutation on ACh sensitivity (at constant Ca^{2+} concentrations) are still not settled. Bertrand *et al.* (2002) report that the human $\alpha4$(S248F), $\alpha4$(776ins3), $\alpha4$(S252L) and $\beta2$(V287M) ADNFLE mutations increase ACh sensitivity. However, Weiland *et al.* (1996) and Bertrand *et al.* (2002) report only a slight leftward shift in the $\alpha4$(S248F) ACh concentration–response relationship relative to the WT, and Kuryatov *et al.* (1997) report a shift in the opposite direction. Also, our results and those of a previous study (Matsushima *et al.* 2002) show that the rat S256L mutation shifts the ACh concentration–response relationship only marginally to the left. Despite such differences, our results and those of Figl *et al.* (1998) show that all five rat ADNFLE orthologues produce a leftward shift in the ACh concentration–response relationship at ACh concentrations $\geqslant$ 30 μM.

It is unclear whether a gain of function based solely on an increase in ACh sensitivity could account for the ADNFLE seizures. If central cholinergic nerve terminals release nearly saturating ACh concentrations (as other types of central synapses apparently do (reviewed in Clements, 1996)), then increasing the ACh sensitivity of $\alpha4\beta2$ nAChRs may only slightly increase the amplitude of nicotinic synaptic potentials. Another problem is that $\alpha4$(S248F)-mediated reductions in the maximum ACh response and single-channel conductance (Kuryatov *et al.* 1997; Bertrand *et al.* 1998; Figl *et al.* 1998) could negate any gain in the synaptic potential amplitude produced by greater ACh sensitivity. Interestingly, a knock-in mouse with an $\alpha4$ mutation that increases ACh sensitivity reduces the threshold for nicotine-induced seizures (Fonck *et al.* 2003), but it is unclear whether this mouse exhibits spontaneous seizures.

The ADNFLE mutations have a number of other pharmacological and biophysical effects on $\alpha4\beta2$ nAChRs not shared by all the mutations. For example, some mutations induce use-dependent potentiation of the 100 nM ACh response, delay the rising phase of the 5–30 nM ACh response (Figl *et al.* 1998), increase the apparent rate of ACh-induced desensitization (Weiland *et al.* 1996; Kuryatov *et al.* 1997; Figl *et al.* 1998; Bertrand *et al.* 2002; Matsushima *et al.* 2002), reduce the maximum ACh response (Kuryatov *et al.* 1997; Figl *et al.* 1998), increase choline sensitivity (Bertrand *et al.* 2002), reduce Ca^{2+} permeability (Kuryatov *et al.* 1997), reduce the single-channel conductance (Kuryatov *et al.* 1997; Figl *et al.* 1998), and alter the voltage-jump relaxation time constants (Figl *et al.* 1998). Also, the $\alpha4$(S248F), $\alpha4$(776ins3) and $\alpha4$(S252L) mutations reduce the half-maximal inhibitory concentration (IC_{50}) of ACh-induced desensitization (Bertrand *et al.* 1998, 2002). However, similar effects have not been reported for the other

ADNFLE mutations, and ACh-induced desensitization is probably too slow to affect nicotinic synaptic transmission under normal physiological conditions (Edmonds *et al.* 1995).

Ca^{2+} both potentiates and blocks neuronal AChRs

Extracellular Ca^{2+} has a dual effect on neuronal nAChRs. At concentrations of 1–8 mM, it potentiates the ACh response (Mulle *et al.* 1992; Vernino *et al.* 1992; Galzi *et al.* 1996), but at concentrations of 10–20 mM, it blocks the human $\alpha4\beta2$ ACh response (Buisson *et al.* 1996). Consistent with previous results for $\alpha7$ nAChRs (Galzi *et al.* 1996), our results show that a single mutation in the $\alpha4$ N-terminal domain (E180Q) abolishes 2 mM Ca^{2+}-induced increases in the $\alpha4\beta2$ ACh response. Thus, the residues that mediate Ca^{2+}-induced increases in the $\alpha4\beta2$ ACh response apparently lie in the N-terminal domain. Because the residues that mediate the positive allosteric effects of Ca^{2+} and the presently known ADNFLE mutations are in different $\alpha4\beta2$ domains, the ADNFLE mutations probably do not reduce Ca^{2+}-induced increases in the ACh response by sterically hindering Ca^{2+} binding to its potentiation site.

Alternatively, the ADNFLE mutations could reduce Ca^{2+}-induced increases in the $\alpha4\beta2$ ACh response by enhancing Ca^{2+} block of the receptor. The effects of the E180Q/V262M mutation on Ca^{2+} modulation of the $\alpha4\beta2$ ACh response and the effects of the S256L mutation on Ba^{2+} modulation support this alternative. Also, a couple of ADNFLE mutations (S248F, S256L) are located at positions that mediate the open-channel block of muscle nAChRs by QX-222 (Leonard *et al.* 1988; Charnet *et al.* 1990). Ca^{2+} could block $\alpha4\beta2$ nAChRs by binding to a site in the channel pore (channel block) or at some other site. The ACh concentration dependence of the S256L-, V262L- and V262M-mediated reductions in Ca^{2+} potentiation and the locations of the ADNFLE mutations in and around M2 suggest that the mutations enhance channel block by Ca^{2+}.

Open-channel block is a form of uncompetitive inhibition. Uncompetitive antagonists produce little inhibition near the foot of the agonist concentration–response relationship, but as the agonist concentration increases, they inhibit the agonist response more effectively. Thus, uncompetitive (open-channel) Ca^{2+} block could explain the ability of the S256L, V262L and V262M mutations to significantly reduce Ca^{2+} dependence at high ACh concentrations (30 μM), but not at the foot (10 nM, 50 nM) of the ACh concentration–response relationship. In contrast to the S256L, V262L, and V262M mutations, the S252F and +L264 mutations reduce Ca^{2+} dependence equally well at high (30 μM) and low (10 nM, 50 nM) ACh concentrations. Thus, Ca^{2+} may be able to reach its pore-blocking site in these mutations equally well in both the closed and open states. Molecular modelling also suggests that the human $\alpha4$(S248F) mutation should enhance Ca^{2+} channel block of the $\alpha4\beta2$ nAChR (Ortells *et al.* 2002).

The apparent voltage independence of the S252F- and +L264-mediated reductions in Ca^{2+} dependence (Figl *et al.* 1998) and Ca^{2+} block of the WT human $\alpha4\beta2$ receptors (Buisson *et al.* 1996) suggests that the $\alpha4\beta2$ divalent cation binding site lies near the extracellular boundary of the membrane electric field. A glutamate residue (αE262) located near the putative extracellular end of M2 (position 20′ in Fig. 1) mediates the block of muscle nAChRs by extracellular Mg^{2+} (Imoto *et al.* 1988). Thus, the aligning $\alpha4$ glutamate (Fig. 1*A*) could participate in an $\alpha4\beta2$ divalent cation blocking site. All five presently reported ADNFLE mutations reduce side-chain polarity. Such a reduction could draw the M2 helices closer together and constrict the channel pore. Bringing the negatively charged glutamates at position 20 in $\alpha4$ closer together could enhance their affinity for divalent cations (Ortells *et al.* 2002).

If Ca^{2+} blocks open S256L, V262L and V262M channels, does one expect smaller synaptic potentials? Yes, if block proceeds quickly enough. At 0 mV, the bimolecular binding forward rate constant for open-channel blockers to muscle nAChRs is 0.5–5.0 ($\times 10^7$) M^{-1} s^{-1} (Sanchez *et al.* 1986). Assuming a similar rate constant for Ca^{2+} binding to its $\alpha4\beta2$ blocking site, open-channel block by Ca^{2+} would be established within < 0.1 ms and therefore could reduce synaptic currents. If central cholinergic nerve terminals release nearly saturating neurotransmitter concentrations (as GABAergic and glutamatergic terminals do (reviewed by Clements, 1996)), then the effects of the ADNFLE mutations on Ca^{2+} modulation at 30 μM ACh are the ones most relevant to synaptic transmission.

How could a change in Ca^{+} modulation lead to nocturnal frontal lobe seizures?

How might a reduction in the Ca^{2+} dependence of the $\alpha4\beta2$ ACh response lead to nocturnal frontal lobe seizures? Similar to other nocturnal epileptiform discharges (Nobili *et al.* 1999*a*,*b*; Beelke *et al.* 2000; Ferrillo *et al.* 2000; Kostopoulos, 2000; Nobili *et al.* 2000, 2001*a*,*b*), thalamocortical oscillations during phase 2 sleep termed sleep spindles (Steriade *et al.* 1993) could trigger ADNFLE seizures. Presynaptic nAChRs facilitate both excitatory and inhibitory transmitter release in the cortex (reviewed in Wonnacott, 1997). Ca^{2+} modulation may act as a negative feedback mechanism to prevent presynaptic $\alpha4\beta2$ nAChRs at central excitatory synapses from over-stimulating glutamate release during repetitive synaptic firing (Amador *et al.* 1995). If the synchronous, repetitive firing associated with sleep spindles selectively depletes Ca^{2+} from the extracellular space around excitatory synapses (Vassilev *et al.* 1997; Rusakov *et al.* 2003), then presynaptic $\alpha4\beta2$ nAChRs should enhance inhibitory

transmitter release more than excitatory transmitter release during sleep spindles. The resulting enhancement of $\alpha4\beta2$-mediated lateral inhibition over $\alpha4\beta2$-mediated lateral excitation may prevent spindle firing from spreading laterally through the cortex and initiating a partial epileptic seizure in normal individuals. However, because the ADNFLE mutations reduce the Ca^{2+} dependence of $\alpha4\beta2$ nAChRs, the difference between $\alpha4\beta2$-mediated excitatory and inhibitory transmitter release during sleep spindles may be less pronounced in ADNFLE patients than in normal individuals. The resulting enhancement of $\alpha4\beta2$-mediated excitatory transmitter release could allow sleep spindles to spread beyond their normal focus in ADNFLE patients and trigger an epileptic seizure. This hypothesis suggests that carbamazepine inhibits ADNFLE seizures by preventing presynaptic $\alpha4\beta2$ nAChRs from enhancing either excitatory or inhibitory neurotransmitter release. However, only a minority of ADNFLE patients have been mapped and there may be additional ADNFLE mutations outside the M2 domain that could have functional characteristics distinct from those described here.

REFERENCES

Amador M & Dani JA (1995). Mechanism for modulation of nicotinic acetylcholine receptors that can influence synaptic transmission. *J Neurosci* **15**, 4525–4532.

Anand R & Lindstrom J (1990). Nucleotide sequence of the human nicotinic acetylcholine receptor $\beta2$ subunit gene. *Nucleic Acids Res* **18**, 4272.

Beelke M, Nobili L, Baglietto MG, De Carli F, Robert A, De Negri E & Ferrillo F (2000). Relationship of sigma activity to sleep interictal epileptic discharges: a study in children affected by benign epilepsy with occipital paroxysms. *Epilepsy Res* **40**, 179–186.

Bertrand D, Picard F, Le Hellard S, Weiland S, Favre I, Phillips H, Bertrand S, Berkovic SF, Malafosse A & Mulley J (2002). How mutations in the nAChRs can cause ADNFLE epilepsy. *Epilepsia* **43**, 112–122.

Bertrand S, Weiland S, Berkovic SF, Steinlein OK & Bertrand D (1998). Properties of neuronal nicotinic acetylcholine receptor mutants from humans suffering from autosomal dominant nocturnal frontal lobe epilepsy. *Br J Pharmacol* **125**, 751–760.

Buisson B & Bertrand D (2001). Chronic exposure to nicotine upregulates the human $\alpha4\beta2$ nicotinic acetylcholine receptor function. *J Neurosci* **21**, 1819–1829.

Buisson B, Gopalakrishnan M, Arneric SP, Sullivan JP & Bertrand D (1996). Human $\alpha4\beta2$ neuronal nicotinic acetylcholine receptor in HEK 293 cells: a patch-clamp study. *J Neurosci* **16**, 7880–7891.

Charnet P, Labarca C, Leonard RJ, Vogelaar NJ, Czyzyk L, Gouin A, Davidson N & Lester HA (1990). An open-channel blocker interacts with adjacent turns of α-helices in the nicotinic acetylcholine receptor. *Neuron* **4**, 87–95.

Clements JD (1996). Transmitter timecourse in the synaptic cleft: its role in central synaptic function. *Trends Neurosci* **19**, 163–171.

Cohen BN, Figl A, Quick MW, Labarca C, Davidson N & Lester HA (1995). Regions of $\beta2$ and $\beta4$ responsible for differences between the steady state dose-response relationships of the $\alpha3\beta2$ and $\alpha3\beta4$ neuronal nicotinic receptors. *J Gen Physiol* **105**, 745–764.

Covernton PJ & Connolly JG (2000). Multiple components in the agonist concentration-response relationships of neuronal nicotinic acetylcholine receptors. *J Neurosci Methods* **96**, 63–70.

De Fusco M, Becchetti A, Patrignani A, Annesi G, Gambardella A, Quattrone A, Ballabio A, Wanke E & Casari G (2000). The nicotinic receptor $\beta2$ subunit is mutant in nocturnal frontal lobe epilepsy. *Nature Genet* **26**, 275–276.

Deneris ES, Connolly J, Boulter J, Wada E, Wada K, Swanson LW, Patrick J & Heinemann S (1988). Primary structure and expression of $\beta2$: a novel subunit of neuronal acetylcholine receptors. *Neuron* **1**, 45–54.

Edmonds B, Gibb AJ & Colquhoun D (1995). Mechanisms of activation of muscle nicotinic acetylcholine receptors and the time course of endplate currents. *Annu Rev Physiol* **57**, 469–493.

Egelman DM & Montague PR (1999). Calcium dynamics in the extracellular space of mammalian neural tissue. *Biophys J* **76**, 1856–1867.

Ferrillo F, Beelke M & Nobili L (2000). Sleep EEG synchronization mechanisms and activation of interictal epileptic spikes. *Clin Neurophysiol* **111**, S65–73.

Figl A, Viseshakul N, Shafaee N, Forsayeth J & Cohen BN (1998). Two mutations linked to nocturnal frontal lobe epilepsy cause use-dependent potentiation of the nicotinic ACh response. *J Physiol* **513**, 655–670.

Fonck C, Nashmi R, Deshpande P, Damaj MI, Marks MJ, Riedel A, Schwarz J, Collins AC, Labarca C & Lester HA (2003). Increased sensitivity to agonist-induced seizures, straub tail, and hippocampal theta rhythm in knock-in mice carrying hypersensitive $\alpha4$ nicotinic receptors. *J Neurosci* **23**, 2582–2590.

Galzi JL, Bertrand S, Corringer JP, Changeux JP & Bertrand D (1996). Identification of calcium binding sites that regulate potentiation of a neuronal nicotinic acetylcholine receptor. *EMBO J* **15**, 5824–5832.

Gerzanich V, Peng X, Wang F, Wells G, Anand R, Fletcher S & Lindstrom J (1995). Comparative pharmacology of epibatidine: a potent agonist for neuronal nicotinic acetylcholine receptors. *Mol Pharmacol* **48**, 774–782.

Goldman D, Deneris E, Luyten W, Kochhar A, Patrick J & Heinemann S (1987). Member of a nicotinic acetylcholine receptor gene family are expressed in different regions of the mammalian central nervous system. *Cell* **48**, 965–973.

Haghighi AP & Cooper E (2000). A molecular link between inward rectification and calcium permeability of neuronal nicotinic acetylcholine $\alpha3\beta4$ and $\alpha4\beta2$ receptors. *J Neurosci* **20**, 529–541.

Hirose S, Iwata H, Akiyoshi H, Kobayashi K, Ito M, Wada K, Kaneko S & Mitsudome A (1999). A novel mutation of CHRNA4 responsible for autosomal dominant nocturnal frontal lobe epilepsy. *Neurology* **53**, 1749–1753.

Hirose S, Okada M, Kaneko S & Mitsudome A (2000). Are some idiopathic epilepsies disorders of ion channels?: a working hypothesis. *Epilepsy Res* **41**, 191–204.

Imoto K, Busch C, Sakmann B, Mishina M, Konno T, Nakai J, Bujo H, Mori Y, Fukuda K & Numa S (1988). Rings of negatively charged amino acids determine the acetylcholine receptor channel conductance. *Nature* **335**, 645–648.

Ito M, Kobayashi K, Fujii T, Okuno T, Hirose S, Iwata H, Mitsudome A & Kaneko S (2000). Electroclinical picture of autosomal dominant nocturnal frontal lobe epilepsy in a Japanese family. *Epilepsia* **41**, 52–58.

Karlin A & Akabas MH (1995). Toward a structural basis for the function of nicotinic acetylcholine receptors and their cousins. *Neuron* **15**, 1231–1244.

Kavanaugh MP, Christie MJ, Osborne PB, Busch AE, Shen K-Z, Wu YN, Seeburg PH, Adelman JP & North RA (1991). Transmitter regulation of voltage-dependent K^+ channels expressed in *Xenopus* oocytes. *Biochem J* **277**, 899–902.

Kostopoulos, GK (2000). Spike-and-wave discharges of absence seizures as a transformation of sleep spindles: the continuing development of a hypothesis. *Clin Neurophysiol* **11**, S27–S38.

Kuryatov A, Gerzanich V, Nelson M, Olale F & Lindstrom J (1997). Mutation causing autosomal dominant nocturnal frontal lobe epilepsy alters Ca^{2+} permeability, conductance, and gating of human $\alpha4\beta2$ nicotinic acetylcholine receptors. *J Neurosci* **17**, 9035–9047.

Leonard RJ, Labarca CG, Charnet P, Davidson N & Lester HA (1988). Evidence that the M2 membrane-spanning region lines the ion channel pore of the nicotinic receptor. *Science* **242**, 1578–1581.

Marubio LM, del Mar Arroyo-Jimenez M, Cordero-Erausquin M, Léna C, Le Novère N, de Kerchove D'Exaerde A, Huchet M, Damaz MI & Changeux JP (1999). Reduced antinociception in mice lacking neuronal nicotinic receptor subunits. *Nature* **398**, 805–810.

Matsushima N, Hirose S, Iwata H, Fukuma G, Yonetani M, Nagayama C, Hamanaka W, Matsunaka Y, Masatoshi I, Kaneko S, Mitsudome A & Sugiyama H (2002). Mutation (Ser284Leu) of neuronal nicotinic acetylcholine receptor $\alpha4$ subunit associated with frontal lobe epilepsy causes faster desensitization of the rat receptor expressed in oocytes. *Epilepsy Res* **48**, 181–186.

Miledi R & Parker I (1984). Chloride current induced by injection of calcium into *Xenopus* oocytes. *J Physiol* **357**, 173–183.

Monteggia LM, Gopalakrishnan M, Touma E, Idler KB, Nash N, Arneric SP, Sullivan JP & Giordano T (1995). Cloning and transient expression of genes encoding the human $\alpha4$ and $\beta2$ neuronal nicotinic acetylcholine receptor (nAChR) subunits. *Gene* **155**, 189–193.

Mulle C, Léna C & Changeux JP (1992). Potentiation of nicotinic receptor response by external calcium in rat central neurons. *Neuron* **8**, 937–945.

Nobili L, Baglietto MG, Beelke M, De Carli F, De Negri E, Gaggero R, Rosadini G, Veneselli E & Ferrillo F (2001*a*). Distribution of epileptiform discharges during nREM sleep in the CSWSS syndrome: relationship with sigma and delta activities. *Epilepsy Res* **44**, 119–128.

Nobili L, Baglietto MG, Beelke M, De Carli F, De Negri E, Rosadini G, De Negri M & Ferrillo F (1999*a*). Modulation of sleep interictal epileptiform discharges in partial epilepsy of childhood. *Clin Neurophysiol* **110**, 839–845.

Nobili L, Baglietto MG, Beelke M, De Carli F, De Negri E, Tortorelli S & Ferrillo F (2000). Spindles-inducing mechanism modulates sleep activation of interictal epileptiform discharges in the Landau–Kleffner syndrome. *Epilepsia* **41**, 201–206.

Nobili L, Baglietto MG, Beelke M, De Carli F, Veneselli E & Ferrillo F (2001*b*). Temporal relationship of generalized epileptiform discharges to spindle frequency activity in childhood absence epilepsy. *Clin Neurophysiol* **112**, 1912–1916.

Nobili L, Ferrillo F, Baglietto MG, Beelke M, De Carli F, De Negri E, Schiavi G, Rosadini G & De Negri M (1999*b*). Relationship of sleep interictal epileptiform discharges to sigma activity (12–16 Hz) in benign epilepsy of childhood with rolandic spikes. *Clin Neurophysiol* **110**, 39–46.

Ortells MO & Barrantes GE (2002). Molecular modelling of the interactions of carbamazepine and a nicotinic receptor involved in the autosomal dominant nocturnal frontal lobe epilepsy. *Br J Pharmacol* **136**, 883–895.

Phillips HA, Favre I, Kirkpatrick M, Zuberi SM, Goudie D, Heron SE, Scheffer IE, Sutherland GR, Berkovic SF, Bertrand D & Mulley JC (2001). CHRNB2 is the second acetylcholine receptor subunit associated with autosomal dominant nocturnal frontal lobe epilepsy. *Am J Hum Genet* **68**, 225–231.

Picard F, Bertrand S, Steinlein OK & Bertrand D (1999). Mutated nicotinic receptors responsible for autosomal dominant nocturnal frontal lobe epilepsy are more sensitive to carbamazepine. *Epilepsia* **40**, 1198–1209.

Picciotto MR, Zoli M, Rimondini R, Léna C, Marubio LM, Pich EM, Fuxe K & Changeux JP (1998). Acetylcholine receptors containing the $\beta2$ subunit are involved in the reinforcing properties of nicotine. *Nature* **391**, 173–177.

Quick MW & Lester HA (1994*a*). Methods of expression of excitability proteins in *Xenopus* oocytes. In *Methods in Neurosciences*, ed. Conn PM, vol. 19, pp. 261–279. Academic Press.

Quick MW, Simon MI, Davidson N, Lester HA & Aragay AM (1994*b*). Differential coupling of G protein alpha subunits to seven-helix receptors expressed in *Xenopus* oocytes. *J Biol Chem* **269**, 30164–30172.

Rusakov DA & Fine A (2003). Extracellular Ca^{2+} depletion contributes to fast activity-dependent modulation of synaptic transmission in the brain. *Neuron* **37**, 287–297.

Sanchez JA, Dani JA, Siemen D & Hille B (1986). Slow permeation of organic cations in acetylcholine receptor channels. *J Gen Physiol* **87**, 985–1001.

Scheffer IE, Bhatia KP, Lopes-Cendes I, Fish DR, Marsden CD, Andermann E, Andermann F, Desbiens R, Keene D & Cendes F (1995). Autosomal dominant nocturnal frontal lobe epilepsy: a distinctive clinical disorder. *Brain* **118**, 61–73.

Shafaee N, Houng M, Truong A, Viseshakul N, Figl A, Sandhu S, Forsayeth JR, Dwoskin LP, Crooks PA & Cohen BN (1999). Pharmacological similarities between native brain and heterologously expressed $\alpha4\beta2$ nicotinic receptors. *Br J Pharmacol* **128**, 1291–1299.

Steinlein OK, Magnusson A, Stoodt J, Betrand S, Weiland S, Berkovic SF, Nakken KO, Propping P & Bertrand D (1997). An insertion mutation of the CHRNA4 gene in a family with autosomal dominant nocturnal frontal lobe epilepsy. *Hum Mol Genet* **6**, 943–947.

Steinlein OK, Mulley JC, Propping P, Wallace RH, Phillips HA, Sutherland GR, Scheffer IE & Berkovic SF (1995). A missense mutation in neuronal nicotinic acetylcholine receptor $\alpha4$ subunit is associated with autosomal dominant nocturnal frontal lobe epilepsy. *Nature Genet* **11**, 201–203.

Steriade M, McCormick DA & Sejnowski TJ (1993). Thalamocortical oscillations in the sleeping and aroused brain. *Science* **262**, 679–685.

Sutor B & Zolles G (2001). Neuronal nicotinic acetylcholine receptors and autosomal dominant nocturnal frontal lobe epilepsy: a critical review. *Eur J Physiol* **442**, 642–651.

Vassilev PM, Mitchel J, Vassilev M, Kanazirska M & Brown EM (1997). Assessment of frequency-dependent alterations in the level of extracellular Ca^{2+} in the synaptic cleft. *Biophys J* **72**, 2103–2116.

Vernino S, Amador M, Leutje CW, Patrick J & Dani JA (1992). Calcium modulation and high calcium permeability of neuronal nicotinic acetylcholine receptors. *Neuron* **8**, 127–134.

Wadiche JI, Amara SG & Kavanaugh MP (1995). Ion fluxes associated with excitatory amino acid transport. *Neuron* **15**, 721–728.

Weiland S, Witzemann V, Villarroel A, Propping P & Steinlein O (1996). An amino acid exhange in the second transmembrane segment of a neuronal nicotinic receptor causes partial epilepsy by altering its desensitization kinetics. *FEBS Lett* **398**, 91–96.

Wonnacott S (1997). Presynaptic ACh receptors. *Trends Neurosci* **20**, 92–98.

Acknowledgements

This research was supported by the California Tobacco-Related Disease Research Program (6KT-0208), the Epilepsy Foundation (EFA/COHEN-01) and the NIH (NS43800, NS11756). We thank Kira Kostenka for help with the oocytes and Cesar Labarca, Purnima Deshpande, Carlos Fonck, Raad Nashmi, Andrew Tapper, Johannes Schwarz and Jim Boulter for comments.